DFT Study on Nitration Mechanism of Benzene with Nitronium Ion

Litao Chen,[†,‡] Heming Xiao,*[,†] Jijun Xiao,[†] and Xuedong Gong[†]

Department of Chemistry, Nanjing University of Science & Technology, Nanjing 210094, P.R. China, and Institute of Chemical Engineering, Zhejing University of Technology, Hangzhou 310014, P.R. China

Received: February 7, 2003; In Final Form: July 8, 2003

A reaction profile for the nitration of benzene with nitronium ion has been successfully calculated for the first time. Stationary points were located and characterized by the DFT procedures at the B3LYP/ 6-311G** level. When NO_2^+ approaches the benzene molecule, a weakly bound π-complex was first produced, in which the distances between the nitrogen atom of nitronium ion to both carbon atoms C1 and C6 of benzene ring were equal. This bifurcation point was characterized as a transition state leading to a σ-complex reactant by shifting the positive ion to either single carbon C1 or C6. The σ-complex reactant (σ-R) finally reaches to the Wheland intermediate (σ-INT) via a σ-complex transition state (σ-TS). The formation of the σ-TS is the rate-determining step, and the barrier height is 8.37 kJ/mol with the correction for ZPVE. A comparison of the intensities and the shifts given by the computational infrared C−N and C−H stretching frequencies on going from σ-TS to σ-INT shows that the formation of bond C1−N13 and the cleavage of bond C1−H12 are not concerted but stepwise in the process of the nitration. This agrees well with the experimental fact of the lack of kinetic isotopic effect in most aromatic nitration reactions.

1. Introduction

Nitration plays a central role in the theory of aromatic reactivity and is quoted in the textbooks as the canonical example of a mechanistically well-defined electrophilic substitution. Since the classic studies by Ingold and his collaborators,[1] it has been generally accepted that the nitrating agent is usually the nitronium ion, NO_2^+, and that the reaction involves an intermediate σ-complex, called Wheland intermediate.[2] Despite the huge body of data that has been accumulated, the mechanism of aromatic nitration continues to be the subject of active research and some controversy.[1−10] Politzer et al.[3] have computed the properties of some possible intermediate stages in the reactions of benzene and toluene with NO_2^+ by freezing the N−O bond lengths of the NO_2 group at HF/STO-6G and HF/5-31G levels. Gleghorn[4] has optimized five selected benzene−NO_2^+ complexes by HF/4-31G//HF/STO-3G, as well as RMP2/4-31G//HF/4-31G calculations. Yet no reaction pathway was involved for those five complexes. Szabo et al.[5] have finally obtained two energy profiles for the nitration of benzene with two possible protonated methyl nitrate isomers at the HF/3-21G level. The distance between the nitrogen atom of the nitronium ion and the attacked carbon atom was chosen as the reaction coordinate. Points of the reaction profile were located by freezing the reaction coordinate and optimizing the rest of the internal coordinates simultaneously. The profile for benzene with bare (unsolvated) nitronium ion, however, could not be carried out, since no activation barrier was found along the chosen reaction coordinate.

As our continuous interest in nitro-compounds as important energetic materials,[11−16] we embarked on study of the nitration mechanism. Since transition-state structure is the most concerned for the mechanism investigation, searching for the transition states on the corresponding reaction profile is our central objective. We finally obtained all the stationary points, including two transition states, along the benzene nitration pathway with no restriction on internal coordinates by the plausible B3LYP hybrid DFT method with a triple-ζ basis set 6-311G**. Hopefully it would give us a better understanding of the microscopic kinetic nitration process.

2. Computational Details

As we all know, the Hartree−Fock (HF) theory does not take into account the effect of instantaneous electron−electron interaction. Therefore the optimization by Hartree−Fock, especially at the low level, is not practical for the sensitive nitro group-containing system. On the basis of the previous investigations by us[13−17] and by other colleagues,[18−21] it is believed that the B3LYP method[22−24] should be effective in calculating reliable geometries, vibration spectra, and energy properties of many molecular systems with planar structure and electronic delocalization.

Stationary points on the profile were positively identified for minimum energy with no imaginary frequencies and the transition state was with only one imaginary frequency. In addition, intrinsic reaction coordinate (IRC) analysis was carried out for each transition state to make sure that the desired reactant(s) and product(s) be connected to the transition structure obtained. Technically, a rather tight convergence criterion was used for the optimization of the transition states (TSs), due to the flat potentials of geometry parameters describing the conformation of the nitro group relative to the ring system.[25,26]

To evaluate the effect by medium, geometry reoptimizations for each stationary point in different media were calculated by self-consistent reaction field (SCRF)[27] technique. The geometry of complexes in the gas phase was used as an initial guess to start the SCRF optimization. The cavity of radius (a_0) was resorted automatically from quantum mechanical procedures[28−30] and fixed during the optimization.

---

* Corresponding author. E-mail: xiao@mail.njust.edu.cn.

[†] Nanjing University of Science & Technology.

[‡] Zhejing University of Technology.

10.1021/jp030167p CCC: $25.00

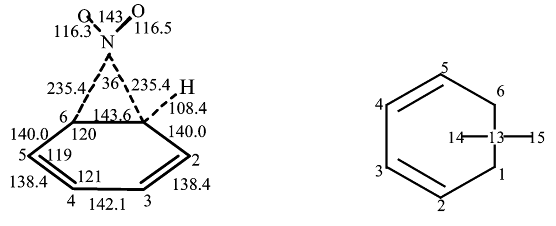

π-complex TS π-complex TS

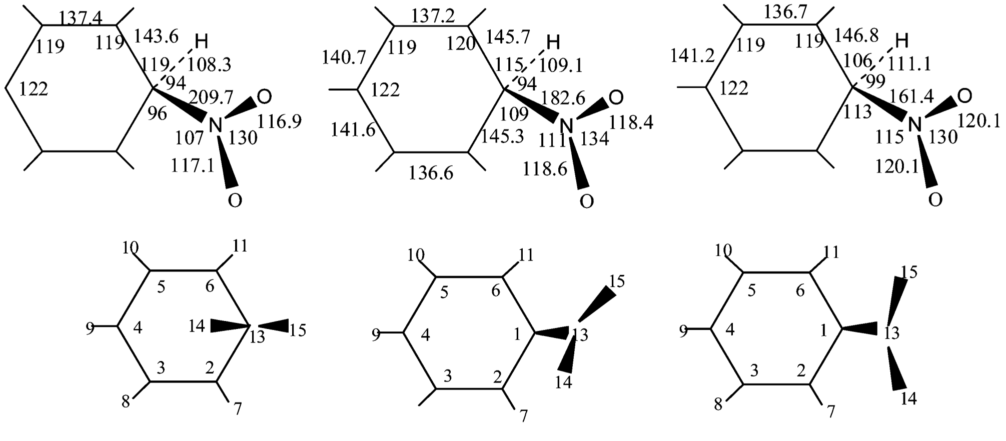

σ - complex R σ - complex TS σ - complex INT

Figure 1. Calculated structures and planforms of R, TSs, amd INT complexes optimized at B3LYP/6-311G** level (bond lengths in pm and angles in degrees).

All the calculations were performed using the Gaussian 98 program package[31] on an α-workstation in our laboratory.

3. Results and Discussion

3.1. Geometries and Bond Orders. Calculated geometries of all stationary points were shown in Figure 1. The initial linear NO_2^+ bent with a trivial change in bond length for all four complexes. The geometry of π-complex TS was a three-membered ring in which the distance of N13−C1 was equal to that of N13−C6. And as a whole, the NO_2 group was above and across the benzene ring with the dihedral angle of $O_{15}N_{13}C_1H_{12}$ ($d_{15-13-1-12}$) in π-complex is $-23.1°$. After shifting the nitro group to a single carbon atom, either C1 or C6, the π-complex TS became a σ-complex reactant (σ-R). So it is an immediate predecessor of σ-R in view of the proceedings.

The structures of three σ-complexes σ-R, σ-TS and σ-INT showed a remarkably consistent pattern with partial loss of aromatic character. The tetrahedral C−C bonds there (C1−C2, C1−C6) are the longest, while those next to them (C2−C3, C5−C6) are the shortest. As NO_2^+ approaches the ring on going from σ-R to σ-INT, the distance of C1−N13 shortened from 209.7 to 161.4 pm, while the angle $\angle N_{13}C_1C_6$ changed from 96° to 113°, and the dihedral angle of $O_{15}N_{13}C_1H_{12}$ ($d_{15-13-1-12}$) varied drastically from 0.0°to 88.8°, as shown in Figure 1. Comparing these geometric parameters with those of σ- TS, it is evident that the σ-TS was structurally a "halfway"[26] transition state along the intrinsic reaction coordinate. In addition, the geometries of both σ-R and σ-INT show that they are roughly in C_{2v} symmetry. The later discussion on the atomic net electronic populations would lead the same conclusion (vide infra).

The tetrahedral C−H bond lengthened from 108.4 (π-TS) to 108.3 (σ-R) to 109.1 (σ-TS) to 111.1 pm (σ-INT), while the corresponding bond orders decreased from 0.4208 to 0.4079 to 0.3911 to 0.3455, respectively. The tetrahedral C−N distance shortened, as expected, from an average 235.4 (π-TS) to 209.7 (σ-R) to 182.6 (σ-TS) to 161.4 pm (σ-INT). Their covalent bond orders increased initially from 0.0564 to 0.1405 to 0.1489, but then decreased to 0.1283 from σ-TS to σ-INT. This shows the interaction between the benzene ring and the NO_2 group in σ-INT has more electrostatic character than that in σ-TS. As Attina et al.[6] once pointed out, ion−molecule reactions are believed to proceed in the gas phase via the preliminary formation of loose complexes, bound by strong electrostatic interactions between the unsolvated reactants. Furthermore, the relatively large value of the tetrahedral C−H bond order in the Wheland intermediate, more than twice as large as that of the C−N bond, implies that the C−H cleavage would not occur in the rate-determining step. This was in full agreement with the fact that no kinetic isotope effect is observed in most aromatic electrophilic substitutions.

3.2. Charges and Dipole Moments. In these complexes, there is a very sizable charge migration from the electron-rich benzene ring to the NO_2 group. Especially for the σ-INT, the original +1 charge of NO_2^+ is finally more than neutralized (−0.049 e).

By examining the r(C−N) in Figure 1 and the charge of nitro group in Table 1 together, one can see that as the NO_2^+ approaches the benzene ring, the $r_{(C-N)}$ shortens on going from π-TS to σ-R, to σ-TS, and to σ-INT (vide ante), while the charge of nitro group drops from 0.340 e, to 0.273 e, to 0.110 e, and finally to −0.049 e. Obviously, there is a good correlation between the reaction coordinate ($r_{(C-N)}$) and the charge migration of nitro group. That is, the closer the NO_2^+ gets to the ring, the more charge migration occurs in the complex. Thus, the magnitude of the charge migration could also show that the π-TS is the immediate predecessor of the σ-R, like that of the reaction coordinate ($r_{(C-N)}$) does (vide ante).

From atomic charge with hydrogen summed into heavy atom we found the tetrahedral carbon in σ-R had negative charge of

TABLE 1: Net Electronic Populations Calculated for the Complexes

atom	π-complex TS		σ-complex R		σ-complex T		σ-complex INT	
C(1)	−0.129	0.060	−0.280	−0.072	−0.239	0.014	−0.118	0.157
H(12)	0.189		0.208		0.253		0.275	
C(2)	−0.018	0.600	0.040	0.798	0.043	0.877	0.001	0.892
H(11)	0.165		0.176		0.197		0.208	
C(3)	−0.048		−0.076		−0.055		−0.039	
H(10)	0.171		0.168		0.173		0.179	
C(4)	−0.048		0.003		−0.004		−0.003	
H(9)	0.171		0.179		0.189		0.196	
C(5)	−0.018		−0.076		−0.050		−0.039	
H(8)	0.165		0.168		0.173		0.179	
C(6)	−0.130		0.039		0.028		0.001	
H(7)	0.189		0.176		0.183		0.208	
N(13)	0.393	0.340	0.377	0.273	0.320	0.110	0.288	−0.049
O(14)	−0.025		−0.056		−0.108		−0.168	
O(15)	−0.028		−0.048		−0.103		−0.168	

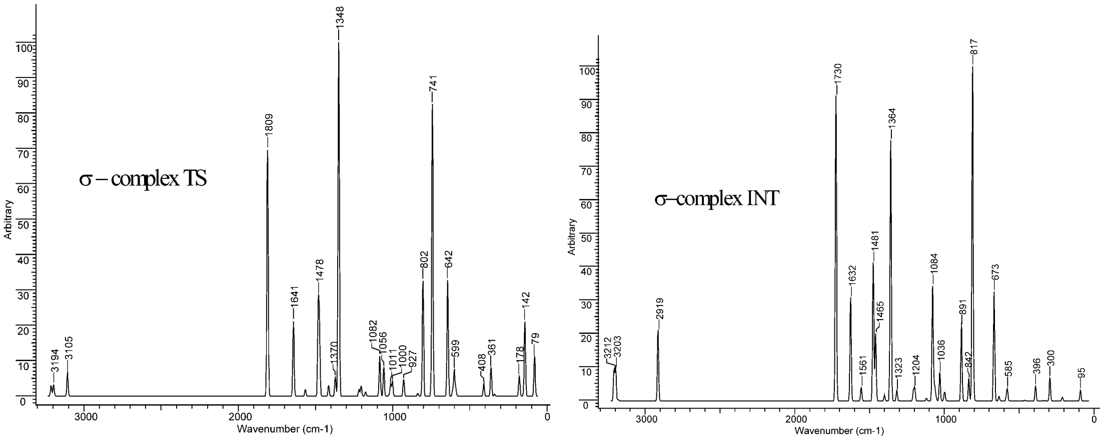

Figure 2. IR Spectra for σ-TS and σ-INT.

TABLE 2: Total Energies and Relative Energies

species	total energy (a.u.)	total energy corrected for ZPVE (a.u.)	relative energies corrected for ZPVE (kJ/mol)	stabilization energies corrected for ZPVE, ΔE_{stab} (kJ/mol)
π-complex TS	−437.132054	−437.019934	2.74	−127.7
σ-complex R	−437.13357	−437.02098	0.0	−130.4
σ-complex TS	−437.13008	−437.01779	8.37	−122.1
σ-complex INT	−437.13266	−437.02008	2.36	−128.1
PhH	−232.30857	−232.20840	130.4	0.0
NO_2^+	−204.77327	−204.76290		

−0.072, yet +0.014 in σ-TS and finally +0.157 in σ-INT. Even the protonated five-membered benzene ring by excluding the tetrahedral carbon still had a charge transfer of ca. +0.1 (0.892−0.798) electron unit from σ-R to σ-INT. This shows the strong electron-withdrawing effect of the nitro group. A total of 0.322 electron unit (−0.049 − 0.273) was withdrawn from the benzene ring by a NO_2 group on going from σ-R to σ-INT, where more than a half of the transferred electronic charge, 0.170, was contributed by hydrogen atoms $\{\sum_{i=7}^{12} H_i(INT) - \sum_{7}^{12} H_i(R)\}$. It is evident that the positive charge of the ring in σ-INT is primarily delocalized over the hydrogen atoms, as shown in Table 1.

The dipole moments of the four complexes of π-TS, σ-R, σ-TS, and σ-INT were 0.777, 1.788, 4.290, and 6.581 D, respectively. The σ-INT and the σ-TS had the larger dipole moment with more separated charge distribution than the former two stationary points. The electrostatic nature of the interaction between the two moieties of benzene ring and nitro group in the TS emphasizes that the S_E2 mechanism, which is classified as a purely ionic process, is preferable for the nitration. Moreover, because of their large dipole moments, it could be predicted that the later two complexes would be greatly influenced by the polar solvents (vide infra).

3.3. Energetics. The energies of species are listed in Table 2. The stabilization energy is defined as $\Delta E_{\mathrm{stab}} = E_{\mathrm{complex}} - (E_{\mathrm{PhH}} + E_{\mathrm{NO_2^+}})$, shown in the last column of Table 2. It is evident that all four complexes are much more stable than the separated reactants (SR). Therefore, their formations are energetically favorable, consistent with a well-known fact that the electrophilic agent NO_2^+ has a strong driving force to interact with other electron-rich aromatics. The π-electrons' delocalization in the complex is partly responsible for the large amount of exothermicity of the nitration of initial reactants, namely the stabilization energy. This may also account for the experimental observation that the nitration of PhH with NO_2^+ is very exothermic and does not require any activation energy.[9] In view of the intrinsic barrier (IB), however, the nitration of benzene with nitronium ion in the gas phase is endothermic,[10] since the energy of INT is 2.36 kJ/mol higher than that of R (see Figure 3). The intrinsic activation barrier is 8.37 kJ/mol. As mentioned earlier, the energy barrier on a potential energy surface is dependent on the both computational method and basis set

TABLE 3: Thermodynamics for the Rate-Determining Step of the Nitration

	σ−complex R			σ−complex TS				
T (K)	C_P^0 (J mol^{-1} K^{-1})	S_m^0 (J mol^{-1} K^{-1})	H_m^0 (kJ mol^{-1} K^{-1})	C_P^0 (J mol^{-1} K^{-1})	S_m^0 (J mol^{-1} K^{-1})	H_m^0 (kJ mol^{-1} K^{-1})	ΔS_T (J mol^{-1} K^{-1})	$k_A \times 10^{-10}$ (mol^{-1} S^{-1})
200.0	93.76	332.46	12.64	84.44	313.97	11.22	−18.49	0.294
298.2	128.50	376.28	23.52	119.06	354.02	21.18	−22.26	1.461
300.0	129.16	377.08	23.76	119.73	354.76	21.40	−22.32	1.489
400.0	163.73	419.06	38.44	154.61	394.07	35.15	−24.99	3.332
500.0	193.16	458.86	56.33	184.38	431.87	52.15	−26.99	5.417
600.0	216.98	496.26	76.88	208.47	467.70	71.84	−28.56	7.528
700.0	236.20	531.20	99.57	227.87	501.34	93.69	−29.86	9.545
800.0	251.91	563.80	124.01	243.71	532.84	117.29	−30.96	11.439

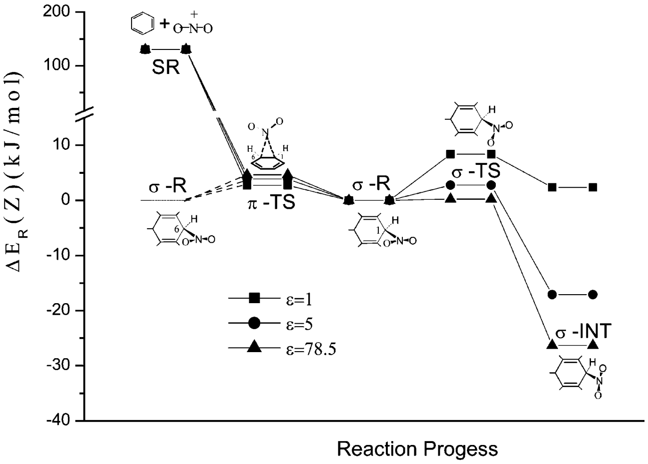

Figure 3. Relative energies for reaction of benzene with nitronium ion in different media.

employed. The absolute value of the energy barrier looks small. Yet a comparison of the relative energies of stationary points could be helpful for us to illustrate the mechanism of the relevant elementary reaction.

3.4. IR Spectra. The B3-based DFT procedures are routinely used to give accurate estimates of experimental fundamentals. It is therefore employed herein as a very cost-effective means of determining harmonic vibrational frequencies and deriving thermochemical quantities. The calculated vibrational frequencies of two complexes presented here were not scaled, because the B3 exchange functional yields scaling factors very close to unity and could often be used directly without resorting to frequency scaling.[35]

It is worthy of noting that there were several weak bands around 3200 cm^{-1} for the C−H stretching vibrations within benzene ring, but a sharper one at 2919 cm^{-1} in the spectrum of σ-INT complex was contributed by the stretching between the tetrahedral carbon and its conjoined H atom. The out-of-plane bending vibration for this CH was at 1084 cm^{-1}. A strong C−N stretching mode was found at 741 cm^{-1} in σ-TS, and at 817 cm^{-1} in σ-INT.[36] This indicates the bond C1−N13 has already partly formed in both σ-TS and σ-INT. A blue shift for this bond stretching frequency on going from σ-TS to σ-INT reflects that the bond strength increases while the bond length decreases (vide ante) during the process. Contrarily, the C−H stretching was weak and its red shift from σ-TS to σ-INT was insignificant, implying the bond C−H would not break in the Wheland intermediate. That is to say, the formation of bond C1−N13 and the cleavage of bond C1−H12 are not concerted, but stepwise in the process of nitration. This accounts for the experimental observation of the lack of kinetic isotopic effect in most aromatic nitration. On the other hands, since the proton would not leave the benzene ring at the rate-determining step, at least one intermediate must be involved in the reaction, consistent with the framework of the S_E2 mechanism.

3.5. Thermodynamics. Since the nitration of benzene usually takes place in solutions, the initial heat of forming the complex is lost instantly to the solvent, without increasing the internal energy of the molecule. It is reasonable to evaluate the standard thermodynamic functions of heat capacities (C_P^0), entropies (S_m^0), enthalpies (H_m^0) for the σ-complexes of R and TS, as well as the change of entropy (ΔS_T) and the rate constant (k_A) for the rate-limiting step of the reaction at each temperature by the statistical thermodynamics and the absolute reaction rate theory.

All the calculated thermodynamic functions were listed in Table 3. It is evident that all the heat capacities and the rate constant (k_A) were increased, while the change of entropy (ΔS_T) was decreased, as expected, with the increasing of temperature. It is worthwhile to note that the rate constant (k_A) demonstrated here was in good agreement with an experimental rate constant of the order of 10^{10} M^{-1} s^{-1}.[8]

3.6. Solvent Effects. Dielectric constants of 1.0, 5.0, and 78.5 were used for the SCRF calculations to represent vacuum (gas phase), nonpolar medium, and aqueous solution, respectively. The changes in relative energy including ZPVE correction in the presence of solvent reaction field for the stationary points of concerned elementary reaction are shown pictorially in Figure 3. Since both σ-TS and σ-INT possess large dipole moments, they are greatly influenced by the polar solvent. As seen in Figure 3, the activation energy of forming σ-TS decreased with the increasing of solvent polarity, while the σ-INT appreciated a great enhancement of stabilization energy. Finally, the formation of σ-TS takes no barrier in the aqueous solution, while the intrinsically endothermic nitration becomes an exothermic reaction. This implies the formation of π-TS would become the rate- determining step in a highly polar medium. Unlike the σ-TS whose relative energy to σ-R is sharply reduced by the increasing dielectric constant, the π-TS is the least influenced complex in solution. As a result, its relative energy to σ-R is oppositely increased, not very much though, with the polarity of the medium.

4. Conclusions

This account reports the full details for nitration of benzene, and the following conclusions can be reached:

1. The geometries of two transition states, π-complex TS and σ-complex TS, have been located and characterized on the potential energy hypersurface for the nitration of benzene with nitronium ion. The profile and the trajectory of the reaction have been then accomplished by the theoretical means.

2. The formation of bond C1−N13 and the cleavage of bond C1−H12 are not concerted, but stepwise in the process of nitration, agreeing with the experimental observation of the lack of kinetic isotopic effect in most aromatic nitrations.

3. At least one intermediate must be involved in the reaction, since the proton would not leave the benzene ring at the rate-determining step. The S_E2 mechanism was then reasonably supposed for the reaction.

4. The degree of charge migration in the σ-TS supports that it is a polar transition state, rather than a radical one.

5. The rate-determining step is the formation of σ-transition state, and the activation energy of this nitration achieved in the gas phase is 8.37 kJ/mol with ZPVE correction at DFT-B3LYP/6-311G** level.

6. The calculations for solvent effects show both σ-transition state and intermediate gain more stabilization energy than other two previous stationary points in aqueous solution for their larger polar moments.

Acknowledgment. We greatly appreciate the support of this work by the National Natural Science Foundation of China (No. 20173028). L. Chen also acknowledges a grant from the Science Center of Zhejiang University of Technology.

References and Notes

(1) Ingold, C. K. *Structure and Mechanism in Organic Chemistry*; Cornell University Press: Ithaca, NY, 1953; Chapter 6.
(2) Wheland, G. W. *J. Am. Chem. Soc.* **1942**, *64*, 900.
(3) Politzer, P.; Jayasuriya, K.; Sjoberg, P.; Laurence, P. R. *J. Am. Chem. Soc*. **1985**, *107*, 1174.
(4) Gleghorn, J. T.; (in part) Torossian, G. *J. Chem. Soc., Perkin Trans. II* **1987**, 1303.
(5) Szabo, K. J.; Hornfeldt, A.-B.; Gronowitz, S. *J. Am. Chem. Soc.* **1992**, *114*, 6827.
(6) Attina, M.; Cacace, F.; Yanez, M. *J. Am. Chem. Soc.* **1987**, *109*, 5092.
(7) Feng, J. K.; Zhen, X. H.; Zerner, M. C. *J. Org. Chem.* **1986**, *51*, 4531.
(8) Ebersonand, L.; Radner, F. *Acc. Chem. Res.* **1987**, *20*, 53.
(9) Morrison, J. D.; Stanney, K.; Tedder, J. M. *J. Chem. Soc., Perkin Trans. II* **1981**, 967.
(10) Perrin, C. L. *J. Am. Chem. Soc.* **1977**, *99*, 5516.
(11) Xiao, H. M. *The Molecular Orbital Theory for Nitro Compounds*; National Defense Industry Press: Beijing, 1993.
(12) Xiao, H. M.; Chen, Z. X. *The Modern Theory for Tetrazol Chemistry*; Science Press: Beijing, 2000.
(13) Zhang, J.; Xiao, H. M.; Gong, X. D. *J. Phys. Org. Chem*. **2001**, *14*, 583.
(14) Xiao, H. M.; Li, J. S.; Dong, H. S. *J. Phys. Org. Chem*. **2001**, *14*, 644.
(15) Li, J. S.; Xiao, H. M.; Dong, H. S. *Chin. J. Chem*. **2000**, *18.6*, 815.
(16) Chen, Z. X.; Xiao, H. M.; Song, W. Y. *J. Mol. Struct. (THEOCHEM)* **1999**, *460*, 167.
(17) Gong, X. D.; Xiao, H. M.; Tian, H. *Int. J. Quantum Chem*. **2002**, *86*, 531.
(18) Becke, A. D. *J. Chem. Phys*. **1993**, *98*, 5648.
(19) Jouhson, B. C.; Gill, P. M. W.; Pople, J. A. *J. Chem. Phys*. **1993**, *98*, 5612.
(20) Laming, G. J.; Termath, V.; Handy, N. C. *J. Chem. Phys*. **1993**, *99*, 8765.
(21) Baushlicher, C. W., Jr. *Chem. Phys. Lett*. **1995**, *246*, 40.
(22) Lee, C.; Yang, W.; Parr, R. G. *Phys. Rev.* B **1988**, *37*, 785.
(23) Miehlich, B.; Savin, A.; Stoll, H.; Preuss, H. *Chem. Phys. Lett*. **1989**, *157*, 200.
(24) Sosa, C.; Lee, C. J. *Chem. Phys*. **1993**, *98*, 8004.
(25) Szabo, K. J.; Hornfeldt, A.-B. *J. Mol. Struct. (THEOCHEM)* **1992**, *258*, 53.
(26) Szabo, K. J.; Hornfeldt, A.-B.; Gronowitz, S. *J. Mol. Struct. (THEOCHEM)* **1992**, *258*, 67.
(27) Tapia, O.; Goscinski, O. *Mol. Phys*. **1975**, *29* (6), 1653.
(28) Wong, W. H.; Frisch, M. J.; Wiberg, K. B. *J. Am. Chem. Soc*. **1991**, *113*, 4776.
(29) Wong, W. H.; Wiberg, K. B.; Frisch, M. J. *J. Am. Chem. Soc*. **1992**, *114*, 523.
(30) Wong, W. H.; Wiberg, K. B.; Frisch, M. J. *J. Am. Chem. Soc*. **1992**, *114*, 1645.
(31) Frisch, M. J.; Trucks, G. W.; Schlegel, H. B.; Scuseria, G. E.; Robb, M. A.; Cheeseman, J. R.; Zakrzewski, V. G.; Montgomery, J. A., Jr.; Stratmann, R. E.; Burant, J. C.; Dapprich, S.; Millam, J. M.; Daniels, A. D.; Kudin, K. N.; Strain, M. C.; Farkas, O.; Tomasi, J.; Barone, V.; Cossi, M.; Cammi, R.; Mennucci, B.; Pomelli, C.; Adamo, C.; Clifford, S.; Ochterski, J.; Petersson, G. A.; Ayala, P. Y.; Cui, Q.; Morokuma, K.; Malick, D. K.; Rabuck, A. D.; Raghavachari, K.; Foresman, J. B.; Cioslowski, J.; Ortiz, J. V.; Stefanov, B. B.; Liu, G.; Liashenko, A.; Piskorz, P.; Komaromi, I.; Gomperts, R.; Martin, R. L.; Fox, D. J.; Keith, T.; Al-Laham, M. A.; Peng, C. Y.; Nanayakkara, A.; Gonzalez, C.; Challacombe, M.; Gill, P. M. W.; Johnson, B. G.; Chen, W.; Wong, M. W.; Andres, J. L.; Head-Gordon, M.; Replogle, E. S.; Pople, J. A. *Gaussian 98*, Revision A.7; Gaussian Inc: Pittsburgh, PA, 1998
(32) Melander L. *Arkiv. Kemi* **1950**, *2*, 211
(33) Lauer, W. M.; Noland, W. E. J. *Am. Chem. Soc*. **1953**, *75*, 3689.
(34) Bonner, T. G.; Bowyer, F.; Williams, G. *J. Am. Chem. Soc.*, **1953**, 75, 2605
(35) Scott, A. P.; Radom, L. *J. Phys. Chem*. **1996**, *100*, 16502.
(36) Joseph, B. L.; Herbert, F. S.; David, A. L. Introduction to Organic Spectroscope; Macmillian Publishing Company: New York & Collier Macmillian Publisher: London, 1987; pp 169−181, 220−221.